Crack Initiation and Propagation in a Martensite-Bainite Steel under Rotating Bending Fatigue

G. Chai* and J. Lindén

AB Sandvik, 811 81 Sandviken, Sweden
guocai.chai@sandvik.com, johan.lindén@sandvik.com

ABSTRACT. *A four-point rotating bending fatigue test has been performed on a martensite-bainite low alloyed steel rod material. The influences of microstructure on the crack initiation and propagation path have been investigated. Subsurface crack initiation was observed in all the samples tested. Most of the crack initiation sites were not located at the internal defects such as inclusions or pores, but at the areas with sizes of 4 to 14 grains in the microstructure (subsurface non-defect crack origin-SNDCO). The sizes of both crack initiation site and "fish eye" increase with decreasing applied stress amplitude. The SNDCO appearances have also changed from more ductile fracture to facet with ridge. This phenomenon was explained using expanded Kitagawa diagrams. The subsurface crack initiation started either in the ferrite phase in bainite due to the intrusion and extrusion process or at grain boundaries due to the stress concentration by the pile-up of dislocation*s. *The transition from shear cracking to tensile cracking led to the formation of crack initiation sites. A "fish eye" type of fracture was followed before the final stage cracking. The influence of microstructure on the fatigue crack initiation and propagation lives was discussed.*

INTRODUCTION

For high cycle fatigue, it is known that fatigue crack initiation mainly starts at surface defects at high stresses or in short fatigue life range, but may shift to the subsurface in long-life range or at cryogenic temperatures [1, 2]. A surface treatment such as shot peening or case hardening may promote this shift.

Subsurface crack initiation mostly starts at internal defects such as inclusions or pores. This phenomenon as an important topic has been widely investigated [1]. However, another type of subsurface crack initiation, which is not associated with pre-existing defects (subsurface non-defect crack origin (SNDCO)), has been reported [2-6]. Titanium alloy is a typical material that shows subsurface crack initiation at the α phase or at the grain boundaries at and below room temperature under cyclic uniaxial loading condition [2- 4]. SNDCO was also observed in some austenitic stainless steels under cyclic uniaxial loading at cryogenic temperature [5] and some surface hardened carbon steels under rotating bending loading [6]. It was pointed out that localised deformation due to dislocation pileup and microstructure imhomogeneity could be the potential sources of microcracking [2]. However, the correlation between the subsurface crack initiation site and the microstructure is still not clear. The purpose of this investigation is therefore to get

a better understanding of the subsurface cracking path, especially the influence of microstructure on the formation of subsurface crack initiation site, its size and morphology and the fatigue life.

MATERIAL AND EXPERIMENTAL PROCEDURE

The material used in this study was a martensite-bainite low alloyed steel rod material with a dimension of 39x12mm, having the base composition as shown in Table 1. Figure 1 shows the typical microstructure and grain structure in the material. The grain size varies from 9 to 25µm.

Table 1. Nominal chemical composition (wt%).

Cr	Ni	Mo	Mn	Si	C
1,3	2,7	0,25	0,65	0,25	0,23

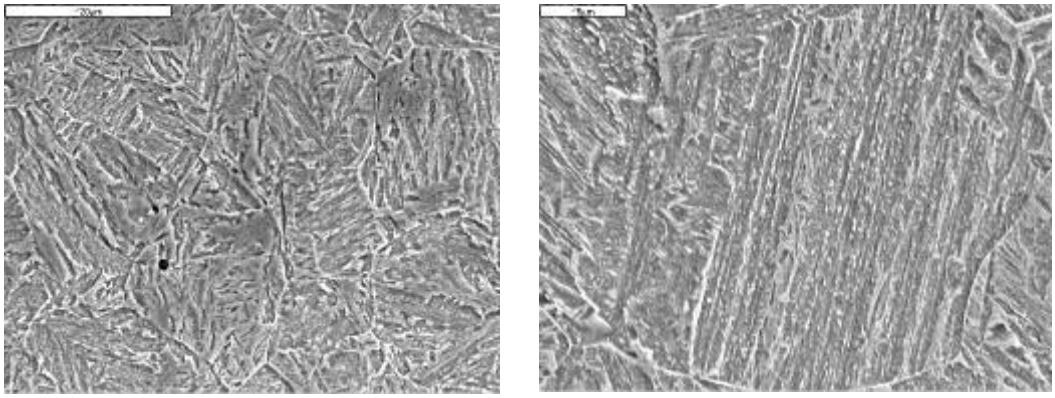

Figure 1. Microstructure and grain structure of the material.

The composition given in Table 1 is typical from the core material, the surface was however casehardened, which led to an increase in hardness at the surface. The tensile properties, measured at room temperature (RT), are summarised in Table 2.

Table 2. Tensile properties of the material at RT.

$R_{p0,02}$ MPa	R_m MPa	A %	Hardness (Hv)
800-1000	1200-1400	15-20	380-440

In order to investigate the fatigue crack initiation, the microstructures and short cracks in the fatigued samples were investigated using both light optical microscopy (LOM) and scanning electron microscopy (SEM). The samples were taken on the both cross and longitudinal sections. The sample from the cross section was taken by just polishing the "fish eye". The longitudinal sample was prepared through the centre of the "fish eye".

The fatigue testing was carried out with a testing set-up for four-point rotating bending fatigue. The as received bar material was used as specimen for testing under a maximum stress level of 350MPa with a frequency of 600rpm or 10Hz.

The fatigue fractures were investigated using scanning electron microscopy (SEM), and the chemical composition at the crack initiation site was analysed by energy disperse spectrometry (EDS).

RESULTS AND DISCUSSION

Formation of Subsurface Crack Initiation Sites

The subsurface crack initiation was observed in all samples. They occurred below the case hardened zone where the hardness is the same as that in the centre. The fatigue fracture is typical "fish eye", which includes the subsurface crack initiation site (Stage I cracking), the crack propagation area (Stage II cracking) and rapid propagation area (final failure) three stages as shown in Figure 2a. In the initiation sites, three types of fracture surfaces have been observed (Figure 2b-2d). In the first two types, no pre-existing defects such as inclusions or pores were detected in the initiation sites. The EDS analysis showed that the composition in this area is similar to that in the matrix. The crack initiation site in Figure 2b, which is nearer the surface, is smaller and contains more tear ridges. The crack initiation site in Figure 2c, which is situated further away from the surface, is bigger and facet. Subsurface crack initiation at inclusion was also observed (Figure 2d). However, it was the only one observed in this investigation.

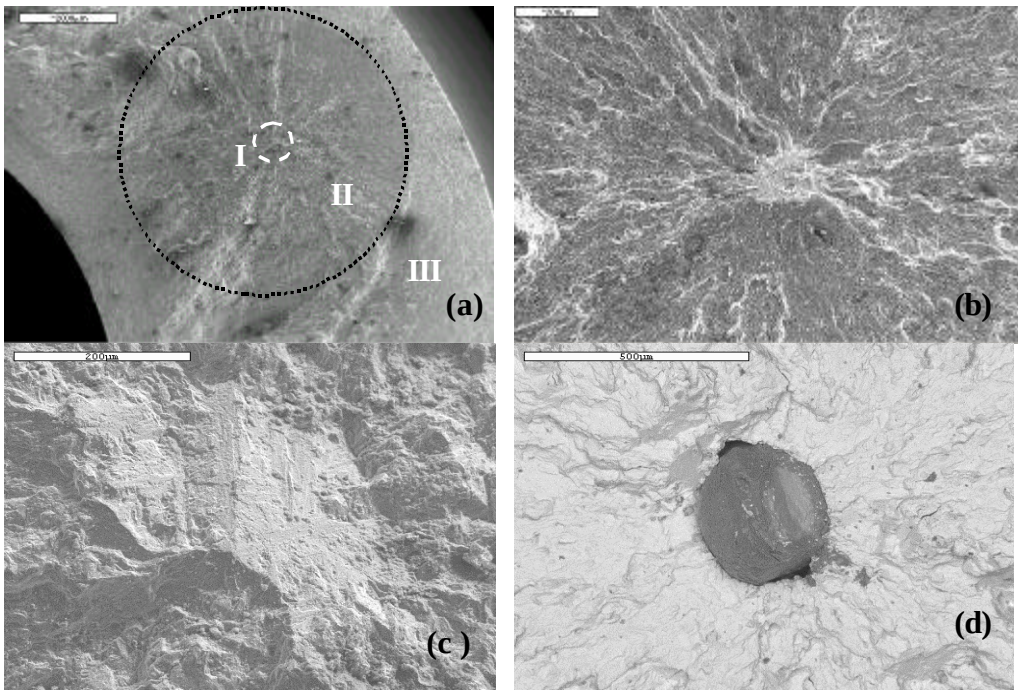

Figure 2. SEM micrographs of the fracture surfaces: (a). Overview of the fracture, (b). Crack initiation site near the surface, (c). Crack initiation site away from the surface, (d). Inclusion as crack initiation site.

As mentioned previously, the size of SNDCO varied with its location. This phenomenon was also reported by Umezawa et al. [5]. However, the morphology of SNDCO has also changed from more ductile fracture to facet with ridge when the position of the SNDCO moved from the surface to the centre (Figure 3).

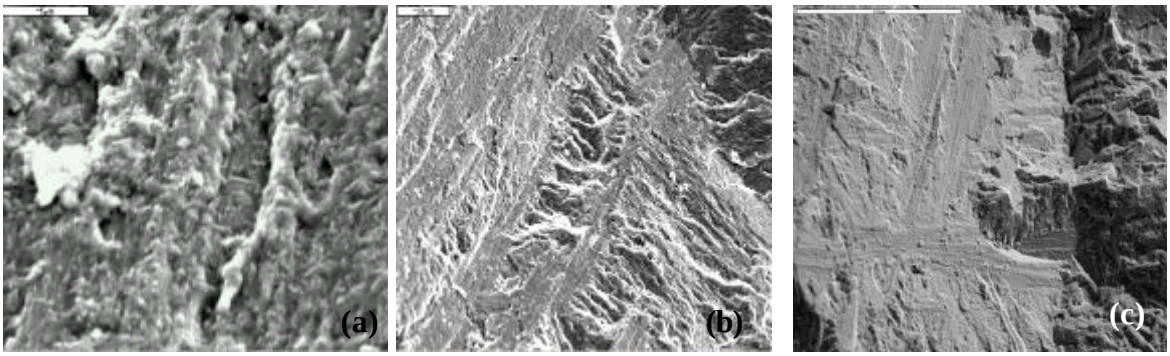

Figure 3. SEM micrographs of the fractures in SNDCO: (a). Martensite lath, (b). Colony facet with martensite lath, (c). Facet with ridge.

Table 3. Summary of the fatigue testing results.

Sample No	Crack origin	Distance (mm)	Size of initiation site (μm)	Size of "fish eye" (mm)	fatigue life (cycles)
1	Martensite lath	1,1	90	2,8	321121
2	Martensite lath	1,2	145	2,2	294858
3	Martensite lath	2,2	154	3,5	525350
4	facet	5,1	220	6,5	372661
5	facet	3,8	171	5,5	344855
6	**inclusion**	**5,3**	318	**7,0**	**254791**
7	Colony facet	4,2	195	6,2	331834
8	Martensite lath	1,8	180	2,8	381302
9	Martensite lath	1,8	162	3,2	394146
10	facet	2,1	193	4,0	459100
11	Colony facet	3,0	225	5,0	367037
12	Colony facet	3,3	239	4,8	451173
13	Colony facet	3,1	164	4,4	500084
14	Colony facet	3,5	196	4,8	517825
15	facet	3,6	128	6,2	347000
16	Colony facet	3,4	134	4,2	385421
17	Colony facet	2,3	131	4,2	560520
18	Martensite lath	2,1	155	4,2	302189

Table 3 shows a summary of the testing results from this investigation. The size of SNDCO and “fish eye” strongly depends on the distance to the surface, and increases with increasing the distance (Figure 4a and 4b). It may be due to the fact that the stresses decrease from the surface to the center in the case of rotating bending fatigue. The

expanded Kitagawa diagrams shown in Figure 4c and 4d may give a qualitative explanation on this.The Kitagawa diagram [7] describes the correlation between the critical crack length and the threshold value of the stress intensity factor range for crack propagation or the fatigue limit. This concept may be used to determine the critical crack length for Stage I cracking (crack initiation site) and Stage II cracking ("fish eye"), and is given by the following equations.

$$\Delta K_{max} = F \Delta\sigma_{max} \sqrt{\pi a} \quad \text{and} \quad \Delta\sigma_{max}=k\Delta\sigma_{max\text{-}surf} \qquad (1)$$

where ΔK_{max} is the maximum stress intensity factor range, F is the geometry factor, $\Delta\sigma_{max}$ is the maximum stress amplitude at a given position in the rod section. , $\Delta\sigma_{max\text{-}surf}$ is the maximum stress amplitude at the rod surface, k is the factor related to the stress decrease in the rod,

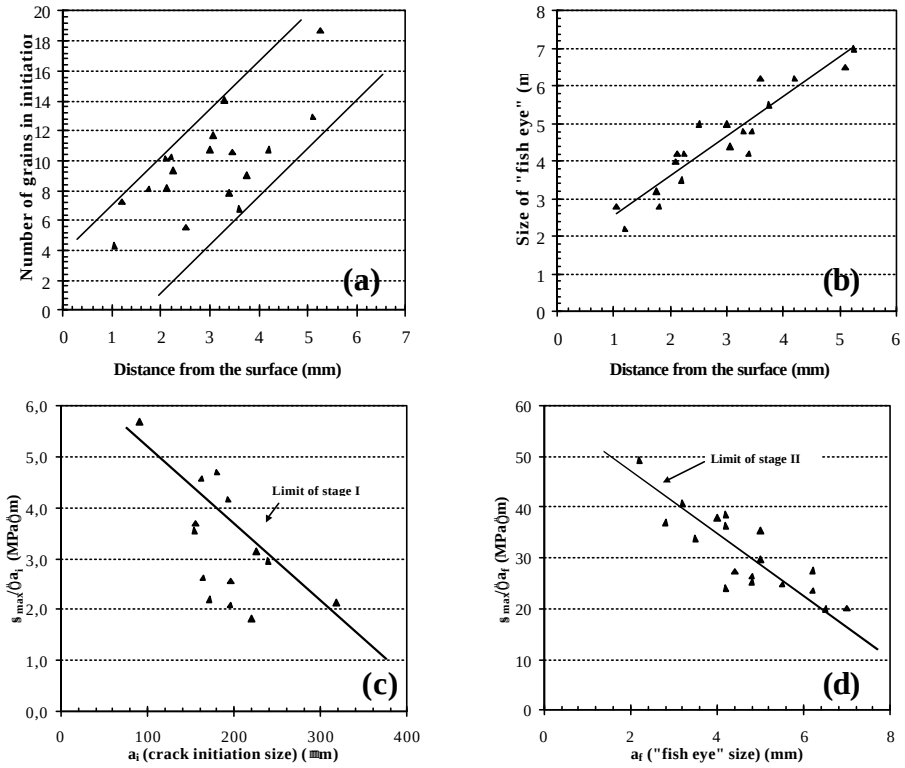

Figure 4. Influence of location on the SNDCO and "fish eye" size: (a). SNDCO size, (b). "fish eye" size, (c). Expanded Kitagawa diagram for Stage I cracking, (d). Expanded Kitagawa diagram for Stage I cracking.

Crack Initiation and Propagation

As shown in Figure 2, the fatigue cracks started at initiation sites. A further SEM investigation showed that cracks may have already been formed, and then propagated at some angle to the fracture surface before the crack initiation sites were formed (Figure 5a and 5b). This indicates that the crack propagation started with shear cracking, and then

propagated parallel to the fracture surface, which led to the formation of crack initiation site. This period is usually defined as Stage I cracking.

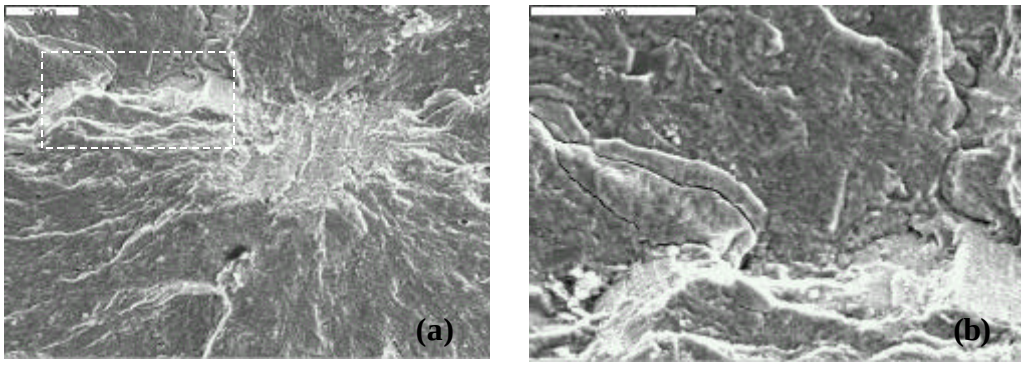

Figure 5. (a). Subsurface crack initiation, (b). Enlarged figure 5a.

The investigation on the "fish eye" shows that the subsurface crack initiation site was located in the area where the hardness was relatively low (Figure 6a) or it contained some coarse ferrite phases that is comparatively soft (Figure 6b).

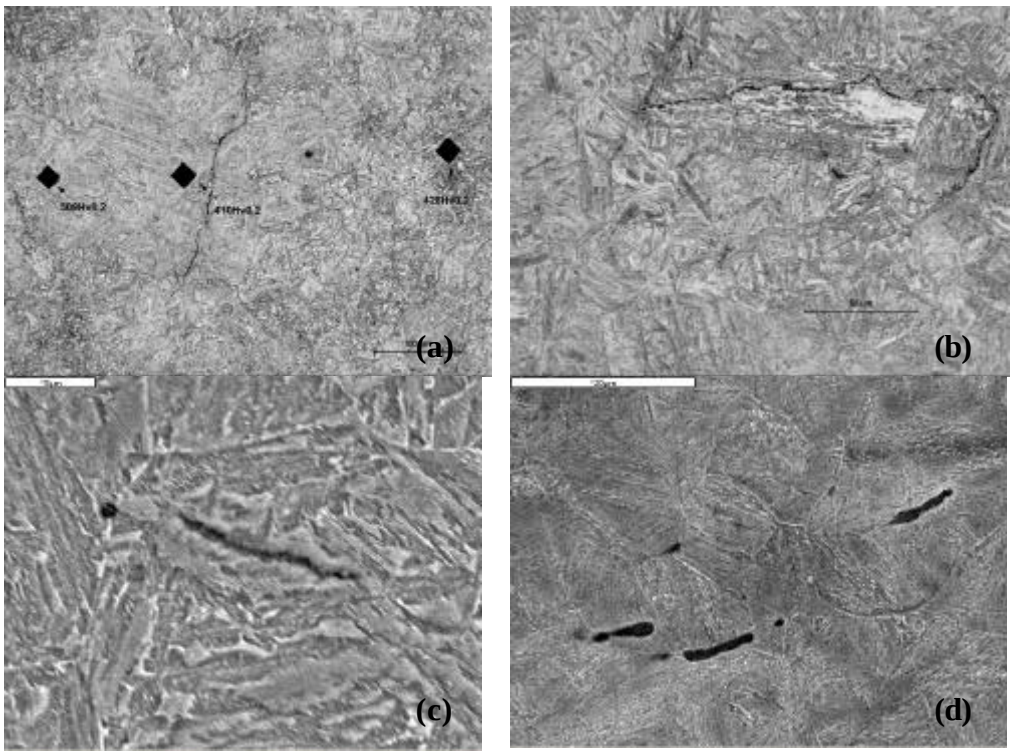

Figure 6. Crack formation: (a) and (b), Crack under "fish eye", (c). Crack in ferrite phase in bainite, (d). Cracks at grain boundaries.

The short-crack investigation on the cross and longitudinal sections showed that the cracks actually started either in the ferrite phase in bainite (Figure 6c) or at grain

boundaries (Figure 6d). This indicates that the formation of a crack was caused either by the intrusion and extrusion process in the ferrite phase in bainite or by the stress concentration due to the pile-up of dislocations near the grain boundaries. Therefore, a possible crack formation mechanism for SNDCO can be:

1). Formation of cracks in the ferrite phases in bainite due to the intrusion and extrusion process or at the grain boundaries by the pile-up of dislocations.
2). A transition from shear cracking to tensile cracking then leads to the formation of crack initiation site (Stage I cracking).

Influence of Microstructure on Fatigue Life

In this investigation, the tests were performed under the same stress condition. However, the fatigue life varied from $2{,}54 \times 10^5$ cycle to $1{,}08 \times 10^6$ cycles. Since the difference of the core hardness in the material is small, the microstructure may have an important effect on the fatigue life. Figure 7a shows the influence of grain size on the fatigue life. As expected, the fatigue life is longer in the material with smaller grain size. However, the fatigue life is shorter if the crack initiation site is an inclusion. In order to investigate the influence of fatigue crack initiation and propagation on the fatigue life, the influence of the number of grains in the SNDCO and the "fish eye" on the fatigue life was studies (Figure 7b and 7c). It shows that the fatigue life increases with increasing number of grains in the SNDCO or in the "fish eye" up to about 300 grains. These results are expected. During the formation process of the SNDCO, the microstructural fracture mechanics (MEM) will dominate. This means that the grain boundaries become the barriers for fatigue crack propagation. Consequently, the fatigue life increases with increasing number of grains. With further increase in crack length, the elastic-plastic fracture mechanics (EPFM) or even linear and non-linear elastic fracture mechanics become dominant, and the grain boundaries as barrier become less important.

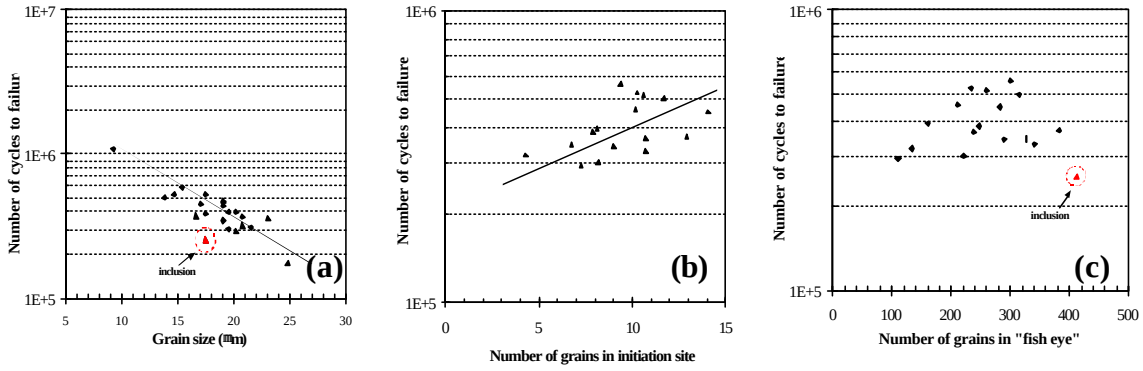

Figure 7. Influence of grain size on the fatigue life: (a). Grain size, (b), Number of grains in SNDCO, (c). Number of grains in "fish eye".

The difference in the fatigue lives started at an inclusion and a non-defect origin mainly depends on the fatigue crack initiation life. According to a dislocation model proposed by Mura et al. [8, 9], the fatigue crack initiation life at a grain boundary and at an inclusion is

given in equation 2 if the shear modulus is assumed to be the same for both inclusion and the matrix.

$$\frac{N_{i\_GB}}{N_{i\_Inc}} = \frac{a_i}{2l} \tag{2}$$

where N_{i_GB} is the crack initiation life at a grain boundary. N_{i_Inc} is the crack initiation life at an inclusion, a_i is the inclusion size, l is the semi-length of slip band. Since a_i usually is larger than l, it can be expected that N_{i_GB} is larger than N_{i_Inc}.

CONCLUSIONS

Subsurface crack initiation occurred both at non-defect areas and at inclusions. The fatigue life is higher if the crack initiation site is a non-defect crack origin, and larger number of grains in the SNDCO.

The SNDCO size and the "fish eye" size increase with decreasing applied stress. This causes also a change in the morphology of SNDCO from more ductile to facet.

The SNDCO starts with cracking either at the ferrite phase in bainite or at grain boundaries, and then the crack has a transition from shear cracking to tensile cracking, which leads to the formation of a crack initiation site (Stage I cracking).

ACKNOWLEDGEMENTS

This paper is published by permission of AB Sandvik. The support of Dr Thorvaldsson T and Mr Lundström M, and the technical assistance of Mr Eriksson T and Mr Lindqvist J are gratefully acknowledged.

REFERENCES

1. Murakami, Y. (2002) *Metal Fatigue: Effect of small defects and nonmetallic inclusion*, Elservier.
2. Umezawa, O. and Nagai, K. (1997) *ISIJ International*. **37**, 1170-1179.
3. Notkina, E., Lütjering, G. and Gysler, A. (2001) In: *Fatigue in the very high cycle regime*, pp. 149-156, Stanzl-Tschegg, S. (Ed.), BOKU, Vienna.
4. Yokoyama, H. et al. (1997) *ISIJ International*. **37**, 1237-1244
5. Umezawa, O. and Nagai, K. (1998) *Metall. Mater. Trans*. **29A**, 809-822.
6. Komotori, J. et al. (2001) *Inter. J. Fatigue*, **23,** 225-230.
7. Kitagawa, H. and Takahashi, S. (1981) In: Proc. 2nd *Inter. Conf. on Mechanical Behavior of Material*, pp. 627-631. Metal Park.
8. Tanaka, K. and Mura, T. (1981) *Trans ASME J Appl. Mech.* **48,** 97-103.
9. Zhou, R. S., Cheng, H. S. and Mura, T. (1989) *Trans ASME J Tribol.* **111,** 605-613.